Supplementary Information

Key Factors behind the Superior Performance of Polymer-Based NFA Blends

Elifnaz Sağlamkaya[1], Mohammad Saeed Shadabroo[1], Nurlan Tokmoldin [1,2], Tanner M. Melody[3], Bowen Sun[1], Obaid Alqahtani[3,4], Acacia Patterson[3], Brian A. Collins[3], Dieter Neher[1], Safa Shoaee[1,2]*

1. Institute of Physics and Astronomy, University of Potsdam, Karl-Liebknecht-Str. 24-25, 14476 Potsdam-Golm, Germany. E-mail: shoai@uni-potsdam.de
2. Paul-Drude-Institut für Festkörperelektronik Leibniz-Institut im Forschungsverbund Berlin e.V., Hausvogteiplatz 5-7, 10117 Berlin, Germany,
3. Department of Physics and Astronomy, Washington State University, 100 Dairy Road, Pullman, WA, 99164 USA
4. Department of Physics, Prince Sattam bin Abdulaziz University, Alkharj, 11942, Kingdom of Saudi Arabia

Experimental section:

Device and sample preparation

The donor polymers PM6 and PM7, the small molecule donor ZR1, the small acceptor molecule Y6, and the electron transport layer PDINN were purchased from 1-Material Inc. The solvents chloroform ($CHCl_3$), methanol (MeOH) and the additive chloronaphthalene (CN) were purchased from Sigma Aldrich. Devices with a regular configuration were fabricated with the structure ITO/PEDOT:PSS/active layer/PDINN/Ag. Patterned ITO (Lumtec) substrates were cleaned in an ultrasonic bath with Hellmanex for 1h, deionized water for 30 minutes, isopropanol for 10 minutes, and acetone for 5 minutes followed by microwave plasma treatment (4 min at 200W). PEDOT:PSS (Clevios AI 4083) was filtered through a 0.2 µm PA filter, spin-coated onto ITO at 5000 rpm, and thermally annealed at 150°C for 15 minutes under ambient conditions, resulting in a 30 nm film. The PM7:Y6(1.1.2) blend was dissolved in CF (0.5% v/v CN) with 16 mg/mL concentration for overnight at room temperature, then heated to 65°C for 30 minutes and spin-coated at 2500 rpm to obtain 100 nm thick active layer followed by annealing at 95°C for 5 minutes. The PM6:Y6 (1:1.2) blend was dissolved in CF (0.5% v/v CN) in 16 mg/mL concentration at 40°C for 4 hours, and spin-coated at 2500 rpm to get 100 nm thick active layer and annealed at 100°C for 10 minutes. ZR1:Y6(1:0.5) was dissolved in pure CF in 15 mg/mL concentration at 50°C for 30 minutes and spin coated at 1500 rpm to obtain 120 nm thick active layer, and annealed at 120°C for 10 minutes. A 0.5 mg/mL PDINN solution in methanol was spin coated at 2500 rpm. and 100 nm of Ag as the top electrode were evaporated under a 10^{-6}-10^{-7} mbar vacuum.

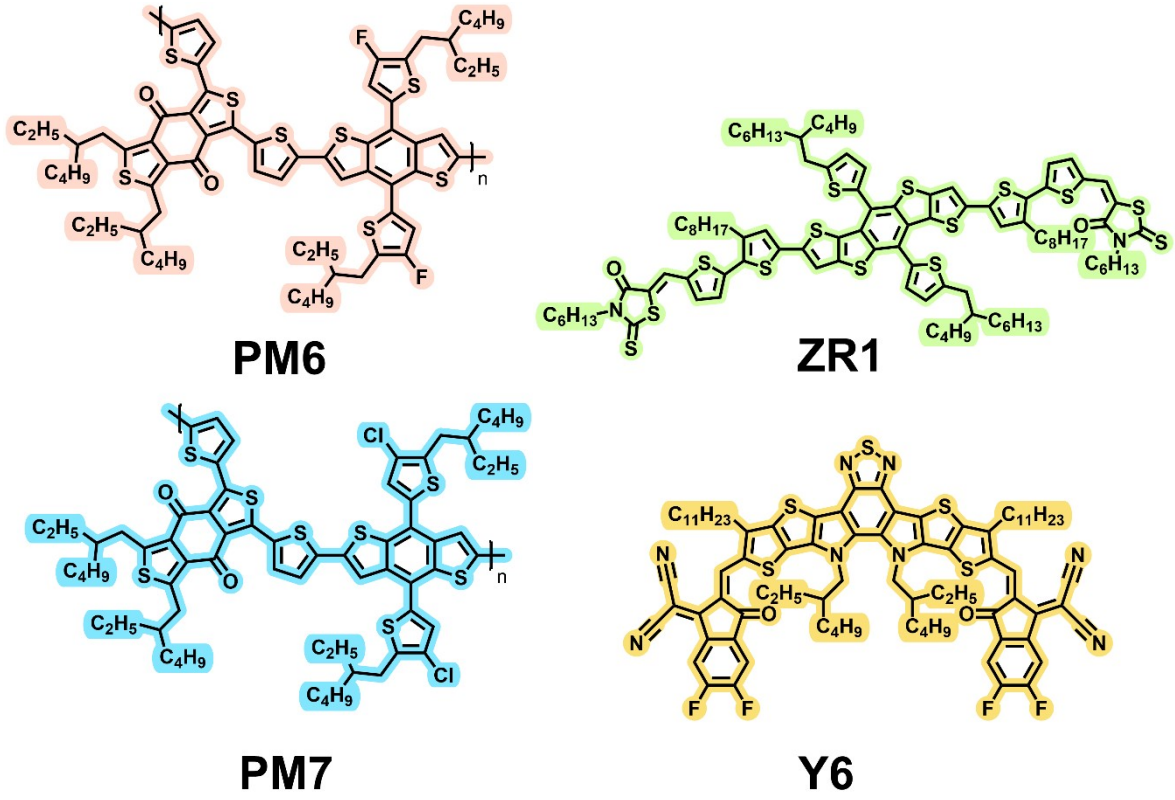

***Figure S1**: Chemical Structures of PM7, PM6, ZR1 and Y6 molecules.*

Current density-voltage characteristics (J-V)

J-V curves were measured using a Keithley 2400 system in a 2-wire source configuration. Simulated AM1.5G irradiation at 100 mWcm-2 was provided by a filtered Oriel Class AAA Xenon lamp and the intensity was monitored simultaneously with a Si photodiode. The sun simulator is calibrated with KG5 filtered silicon solar cell (certified by Fraunhofer ISE).

For temperature-dependent measurements, the devices were loaded into a liquid nitrogen-cooled cryostat (Janis) and the temperature was adjusted in a range of 80 K to 300 K using a temperature controller (Lakeshore 335). J-V data were measured using a Keithley 2400 Source Meter in a two-wire configuration and illumination was done using a white LED. An automated filter wheel was used to measure different intensities.

Quasi-steady-state photoinduced absorption (PIA)

In PIA measurements, the photoexcitation of a 405-nm continuous wave laser diode (Spectral Products) is modulated at a frequency of 570 Hz by an optical chopper (Thorlabs MC2000B). The white light emitted from a tungsten halogen lamp is optically directed into a monochromator (Spectral Products DK240), and the monochromatic light existing from the monochromator is used as the probe light, and focused on the studied device to overlap with the photoexcitation light. The change in the transmitted probe light ΔT induced by the photoexcitation is recorded by a Si photodiode (Thorlabs) and a lock-in amplifier (SR830) and then corrected by a background subtraction. The transmitted probe light T through the unexcited sample is measured by using another optical chopper (Thorlabs

MC2000B) to modulate the probe light, the same photodiodes and the lock-in amplifier. Our PIA system has a sensitivity on the order of 10^{-7}. For temperature-dependent measurements, the devices were loaded into a liquid nitrogen-cooled cryostat (Janis) and the temperature was adjusted in a range of 80 K to 300 K using a temperature controller (Lakeshore 335). J-V data were measured using a Keithley 2400 Source Meter in a two-wire configuration.

Bias-assisted charge extraction (BACE)

In BACE, to establish steady-state conditions, we used a high power 1 W, 445 nm laser diode (insaneware) with a switch-off time of ~10 ns. The laser diode was operated at 500 Hz with a duty cycle of 50%, such that illumination lasted 1 ms and the diode was switched off for also 1 ms. During illumination, the device was held at the equivalent V_{OC} using an Agilent 81150A pulse generator. Right after switching-off the laser, a high reverse was applied to the sample by the same fast pulse generator (Agilent 81150A), allowing a fast extraction time of 10-20 ns. The current transients were measured via a 10 Ω resistor in series with the sample and recorded with an oscilloscope (Agilent DSO9104H). For temperature dependent measurements, the device was placed on the cooling finger of a closed cycle helium cryostat (ARS-CS202-X1.AL). The cryostat was heated and evacuated to $1x10^{-4}$ mbar (Pfeiffer TCP121 Turbo pump and Edwards XDS-10 scroll pump). Electrical connection was done through a home-built amplifier which was directly attached as close as possible to the sample outside the cryostat.

Time-delayed collection field (TDCF)

In TDCF, the device was excited with a laser pulse from a diode pumped, Q-switched Nd:YAG laser (NT242, EKSPLA) with ~5 ns pulse duration at a typical repetition rate of 500 Hz. To compensate for 4 the internal latency of the pulse generator, the laser pulse was delayed and homogeneously scattered in an 85 m long silica fiber (LEONI). Then, charges were generated while the device was held at pre-bias V_{pre}. After a varying delay times, a high reverse bias, V_{coll}, was applied to extract all the charges in the device. V_{pre} and V_{coll} were set by an Agilent 81150A pulse generator through a home-built amplifier, which was triggered by a fast photodiode (EOT, ET-2030TTL). The current flowing through the device was measured via a 10 Ω resistor in series with the sample and recorded with an oscilloscope (Agilent DSO9104H). Great care was taken to avoid free carrier recombination prior to extraction. Therefore, a fast ramp-up (~2.5 ns) of the bias was applied.

Photoluminescence (PL) and PL Quantum Yield

Devices and films in study were excited with 520 nm laser diode (insaneware) and the emission spectra were recorded with an Andor Solis SR393i-B spectrograph with a silicon detector DU420A-BR-DD and an Indium Gallium Arsenide DU491A-1.7 detector. A calibrated Oriel 63355 lamp was used to correct the spectral response. PL spectra were recorded with different gratings with centre wavelengths of 800, 1100, and 1400 nm and merged afterwards. In absolute PL measurements, the same laser was used together with an optical fibre that goes in to the integrating sphere that holds the sample. Measurements were made with 1 sun intensity. The spectral photon density was obtained from the corrected detector signal (spectral irradiance) by division through the photon energy (hv), and the

photon numbers of the excitation and emission were calculated from the numerical integration, using a MatLab code.

Electroluminescence (EL) and EL quantum yield (ELQY)

For EL measurements, the device is hold at a constant voltage, using a Keithley 2400, for 1 s. The emission spectra were recorded with an Andor Solis SR393i-B spectrograph with a silicon detector Indium Gallium Arsenide DU491A-1.7 detector. A calibrated Oriel 63355 lamp was used to correct the spectral response. EL spectra were recorded with different gratings with center wavelengths of 800, 1100, and 1400 nm, and merged afterwards.

For absolute EL measurements, a calibrated Si photodetector (Newport) connected to a Keithley 485 picoampere meter were used. The detector, with an active area of ∼2 cm_2, was placed in front of the measured pixel with a distance <0.5 cm, and the total photon flux was evaluated considering the emission spectrum of the device and the external quantum efficiency of the detector. The injected current was monitored with a Keithley 2400.

Space charge-limited currents (SCLC)

To prepare electron-only devices with the configuration ITO/ZnO/AL/PDINN/Ag, ZnO Nanoparticle dispersion (Sigma Aldrich) were filtered through a 0.45 µm polytetrafluoroethylene filter and spin coated onto ITO at 5000 rpm for 30 s in air. The ZnO substrates were annealed at 120 °C for 30 min. The layers on top of ZnO are prepared as for solar cell devices. Hole-only devices with the configuration ITO/MoO_3/AL/MoO_3/Ag were prepared by evaporating 8 nm of MoO_3 on top of ITO. Then, the active layer was prepared as for solar cell devices, followed by evaporation of 8 nm of MoO_3 under a 10^{-6}-10^{-7} mbar vacuum. For temperature-dependent measurements, the devices were loaded into a liquid nitrogen-cooled cryostat (Janis) and the temperature was adjusted in a range of 80 K to 300 K using a temperature controller (Lakeshore 335). J-V data were measured using a Keithley 2400 Source Meter in a two-wire configuration.

Grazing Incident Wide Angle X-Ray Scattering (GIWAXS) and Resonant Soft X-ray Scattering (RSoXS)

Neat and films were spin-coated on n-doped silicon were prepared for GIWAXS measurements in the optimal device thickness. For RSoX measurements, n-doped silicon substrates were first spin coated with Na:PSS. GIWAXS measurements were acquired with the Xenocs XEUSS 3.0 that utilized a focused Cu source at an incident angle of 0.25 degrees (above the critical angle) with 30 minute exposures. 1D GIWAXS profiles were processed via NIKA software in Igor Pro. RSoXS measurements were conducted on blend films that were floated off of NaPSS sacrificial layers in water onto 100nm thick silicon nitride transmission windows (Noraca). RSoXS was performed at NSLS-ii SST1_7-ID-1 and processed via custom Igor Pro software.

Transmission Electron Microscopy (TEM)

TEM scans were acquired using a FEI Tecnai G2 20 Twin microscope, with a 200KV LaB6 electron gun and a FEI Egal 4k CCD detector. The investigated films were floated off in deionized water then mounted onto TEM copper grids.

Atomic Force Microscopy (AFM)

AFM scans were acquired using a Bruker's Dimension Icon instrument. The surface topology and roughness of the investigated samples were probed with a nitride lever and SCANASYST-AIR silicon tip.

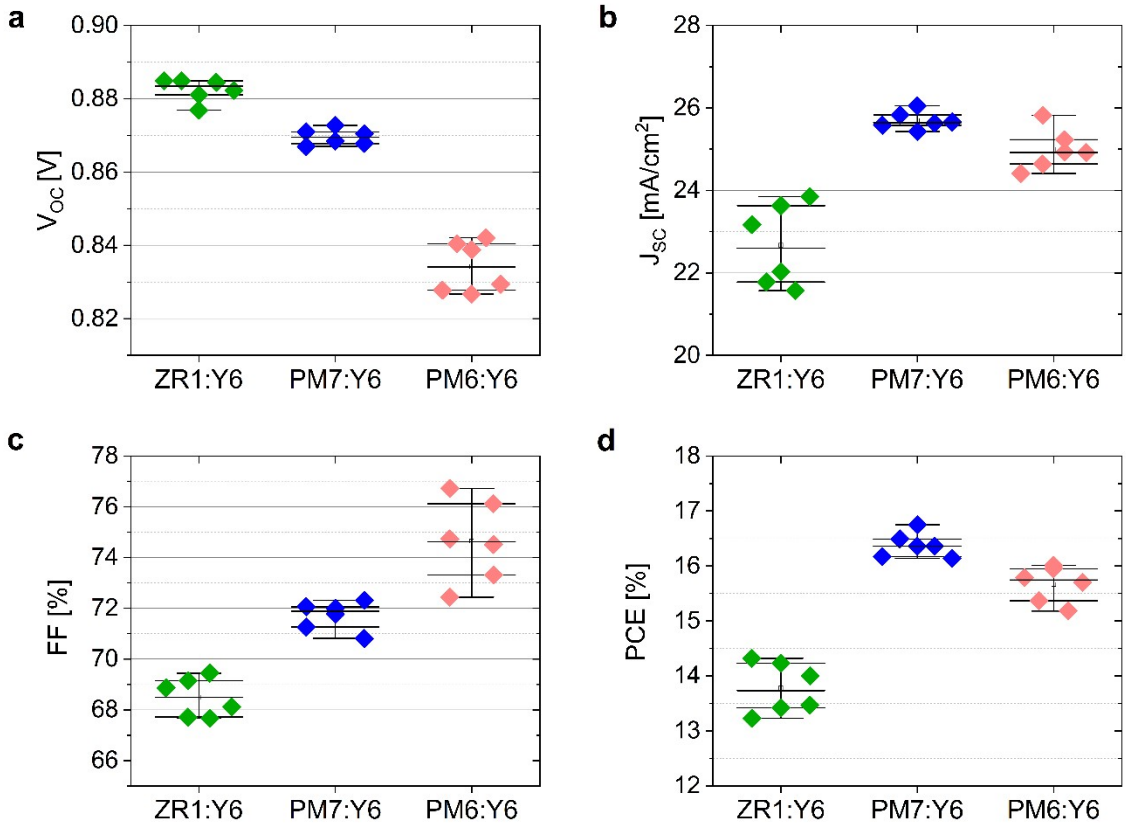

Figure S2: *The average device parameter distributions of PM6:Y6, PM7:Y6 and ZR1:Y6 (of at least 5 individual devices) measured under simulated AM1.5G.*

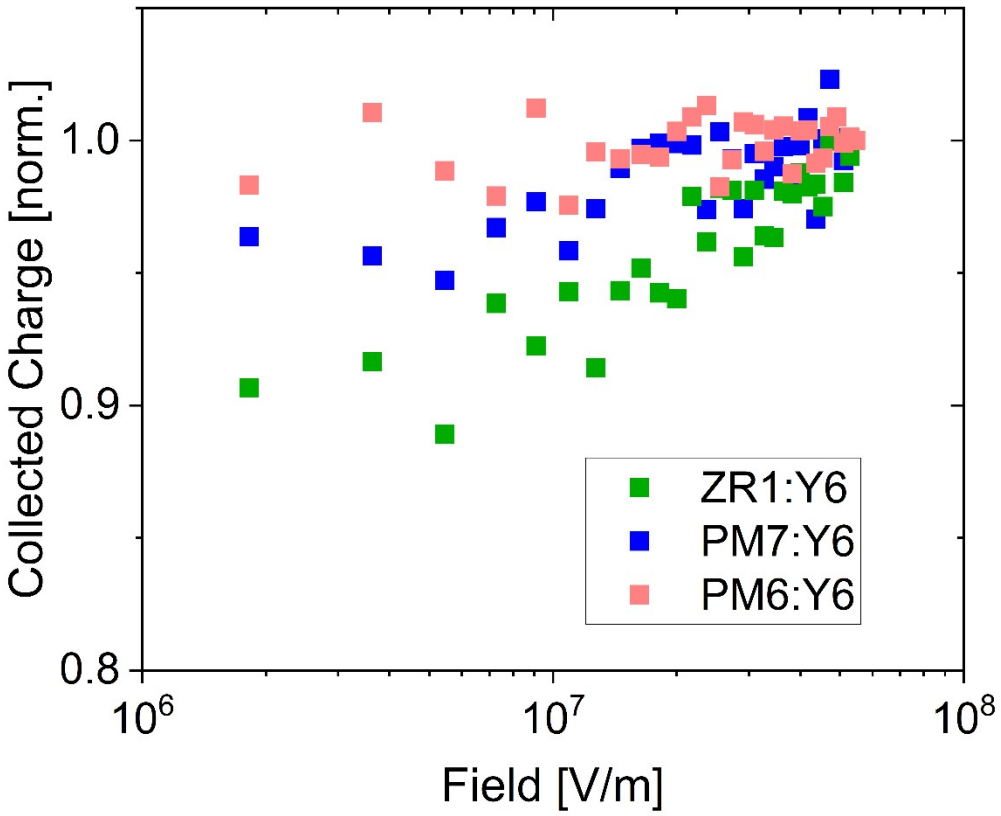

Figure S3: *Collected charge as a function of field is shown measured with time delayed collected field using excitation energy of 2.07 eV and a low fluence of 0.05 μJ cm^{-2}.*

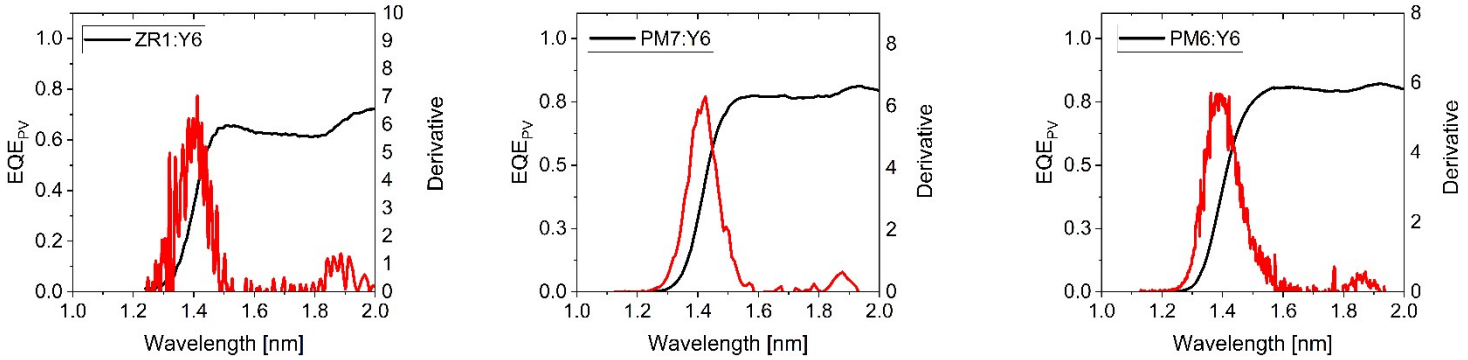

Figure S4: *Derivative of EQE$_{PV}$ spectrum of organic solar cells show similar band-gap of 1.4 eV.*

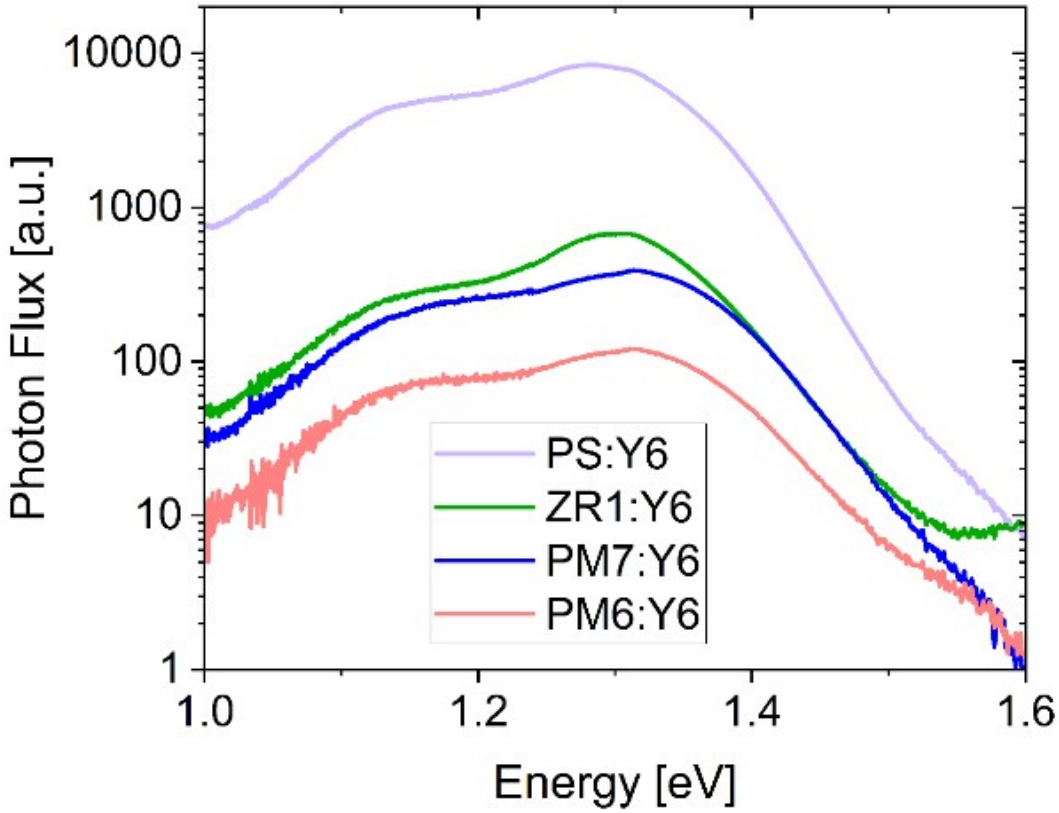

Figure S5. *Photoluminescence spectra of PS:Y6, ZR1:Y6, PM7:Y6 and PM6:Y6 films on glass measured inside an integrating sphere with 2.07 eV excitation energy.*

Table S1 *Photoluminescence quantum yields, and photoluminescence quenching of ZR1:Y6, PM7:Y6 and PM6:Y6 blends are listed. PL quenching percentages were calculated by dividing the PLQY of the blends with the PLQY of the PS:Y6 film.*

	PLQY	***PLQ***
PS:Y6 (1:1 wt.%)	*2.5e-2*	*-*
ZR1:Y6	*1.4e-3*	*94%*
PM7:Y6	*1e-3*	*96%*
PM6:Y6	*3.1e-4*	*99%*

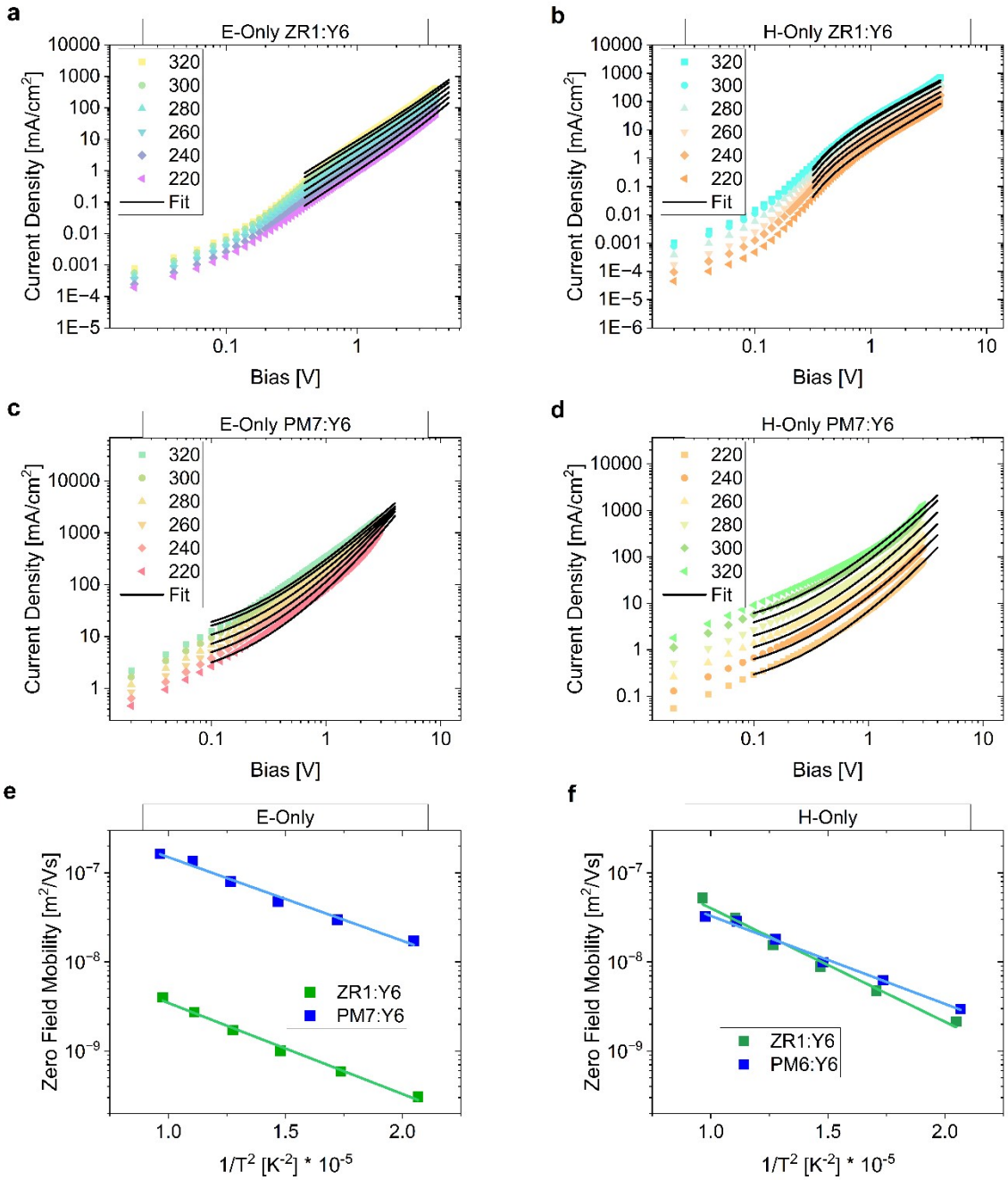

Figure S6. *Temperature dependent SCLC curves of* ***a****) the electron-only,* ***b****) hole-only ZR1:Y6* ***c****) electron only and* ***d****) hole-only and PM7:Y6 devices in 160-170 nm active layer thickness. The temperature dependent zero-field mobilities of* ***e****) the electron-only ZR1:Y6 and PM7:Y6 devices in in ITO/ZnO/AL /PDINN/Ag structure and* ***f****) the hole-only devices in ITO/MoO_3/AL/MoO_3/Ag structure.*

Supplementary Note 1. V_{OC} *as* a function of carrier density and energetic disorder:

Estimation of the band-gap in D and A organic blends is not trivial due to the energetic off-set and the energetic disorder. Especially for small offset systems, the CT energy is not visible in For Gaussian DOS, charge carrier density as a function of Fermi energy can be expressed with the Gauss-Fermi integral. (**Equation S1**). An analytical solution to this equation is not available; nevertheless, it can be approximated to non-degenerate and degenerate expressions for different temperature regimes.

$$\frac{n}{N_0} = \frac{1}{\sigma\sqrt{2\pi}} \int \exp\left(-\frac{1}{2} \frac{(E - E_0)^2}{\sigma^2} \right) \frac{1}{e^{(E - E_F)/k_B T} + 1} dE$$

Equation S1.

Here, n is the carrier density N_0 is density of states, σ is energetic disorder, E is energy and E_0 is the center of DOS, E_F is the Fermi energy, k_B is the Boltzmann constant and T is the temperature in Kelvin. For low carrier densities, most of the states are unoccupied, and Fermi energy of the electrons or holes ($E_{F,e}$, $E_{F,h}$ respectively) is located inside the band-gap of the semiconductor. In this case, there are discrete energy levels and non-degenerate approximation can be used. For organic semiconductors the limit for the non-degenerate region is defined for $E_{F,e}$ below the equilibrium energy (($\varepsilon_{\infty,e} = E_{LUMO} - \frac{\sigma_{LUMO}^2}{k_B T}$) of the electrons, and vica versa for the holes. This transition from non-degeneracy is expressed with for the case $\frac{(E - E_F)}{k_B T} = -\left(\frac{\sigma}{k_B T}\right)^2$.

$$\frac{n}{N_0} = \frac{1}{2}\exp\left(\frac{(E - E_F)}{2k_B T}\right) = \frac{1}{2}\exp\left(-\frac{1}{2}\left(\frac{\sigma}{k_B T}\right)^2 \right)$$

Equation S2.

We used temperature dependent n from our PIA measurements (shown in Figure 2c in manuscript), and for σ, average of σ_{LUMO} and σ_{HOMO} from our SCLC measurements. The corresponding transition temperature was in between 200 and 170 K for both systems.

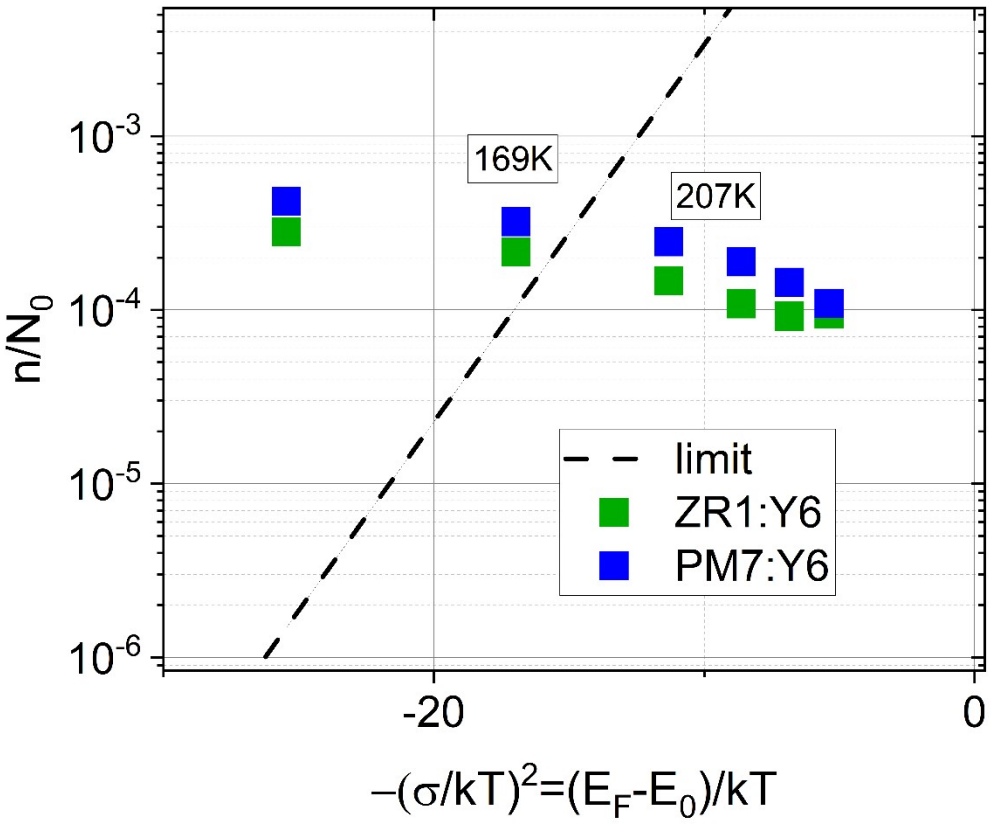

Figure S7. *Relationship between* $\frac{n}{N_0}$ *and energy is shown where the dashed line represents the transition from non-degeneracy to degeneracy given by the Equation S2. The points are the temperature dependent carrier density of the ZR1:Y6 and PM7:Y6 blend systems corresponds to the* $-\left(\frac{\sigma}{k_B T}\right)^2$ *for their SCLC disorder.*

For the degenerate regimes, $E_{F,e}$ and $E_{F,h}$ are calculated as

$$E_{F,e} = E_{LUMO} - \frac{\sqrt{2}\sigma_{LUMO}}{H_{LUMO}} erfc^{-1}\left(2\frac{n}{N_0}\right)$$

$$E_{F,h} = E_{HOMO} + \frac{\sqrt{2}\sigma_{HOMO}}{H_{HOMO}} erfc^{-1}\left(2\frac{n}{N_0}\right)$$

The functions H_{LUMO} and H_{HOMO} are:

$$H_{LUMO} = \frac{\sqrt{2}}{\sigma_{LUMO}} k_B T erfc^{-1}\left[\exp\left(-\frac{1}{2}\left(\frac{\sigma_{LUMO}}{k_B T}\right)^2\right)\right]$$

$$H_{HOMO} = \frac{\sqrt{2}}{\sigma_{HOMO}} k_B T erfc^{-1}\left[\exp\left(-\frac{1}{2}\left(\frac{\sigma_{HOMO}}{k_B T}\right)^2\right)\right]$$

Thereafter, $^{qV_{OC}}$ can be calculated from the difference between $E_{F,e}$ and $E_{F,h}$ for the degenerate case.

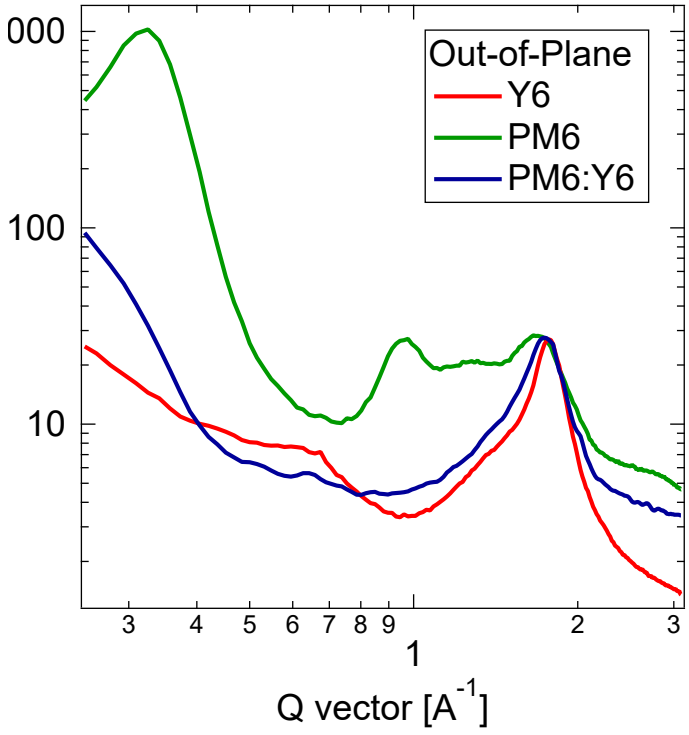

Figure S8. *1D OoP GIWAXS profiles of PM6 (green), Y6 (red), and PM6:Y6 (blue).*

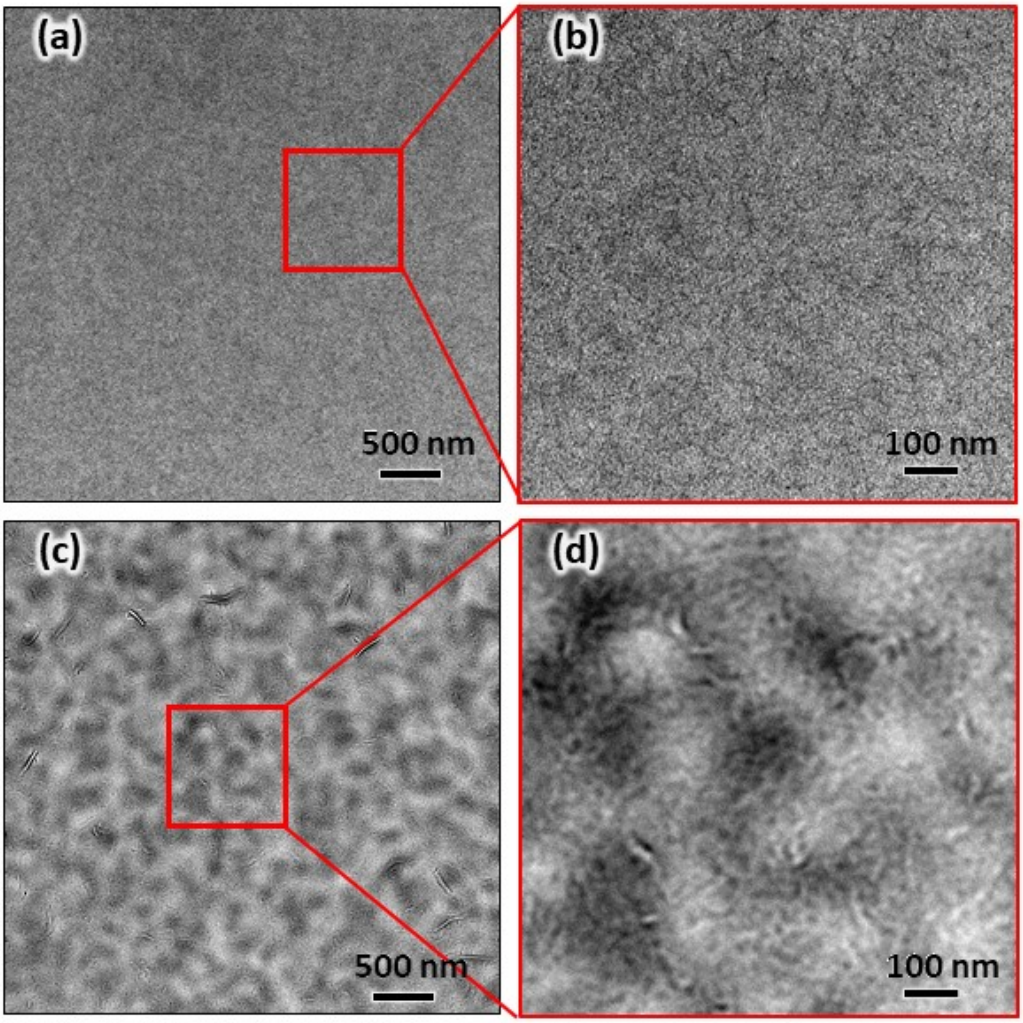

Figure S9. *TEM scans of PM6:Y6 blend (a) and (b); and scans of ZR1:Y6 blend (c) and (d). Scans b and d are zoomed in images of a and c, respectively.*

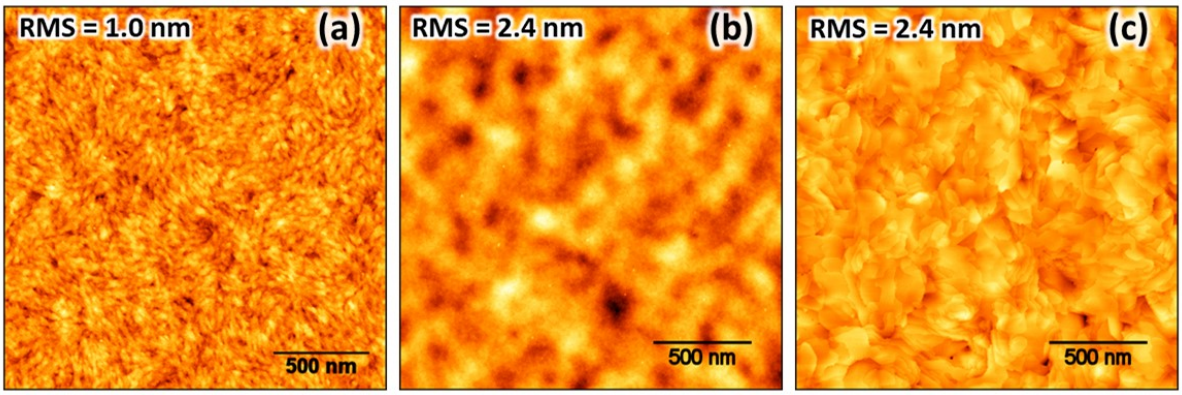

Figure S10. *Atomic force microscopy (AFM) scans of neat films: (a) PM6, (b) Y6 and (c) ZR1. The scale bar in all images is 500 nm. The fibrous surface texture of PM6 is assigned to polymer fibrils. The platelet-like texture of ZR1 is assigned to ZR1 crystallites.*

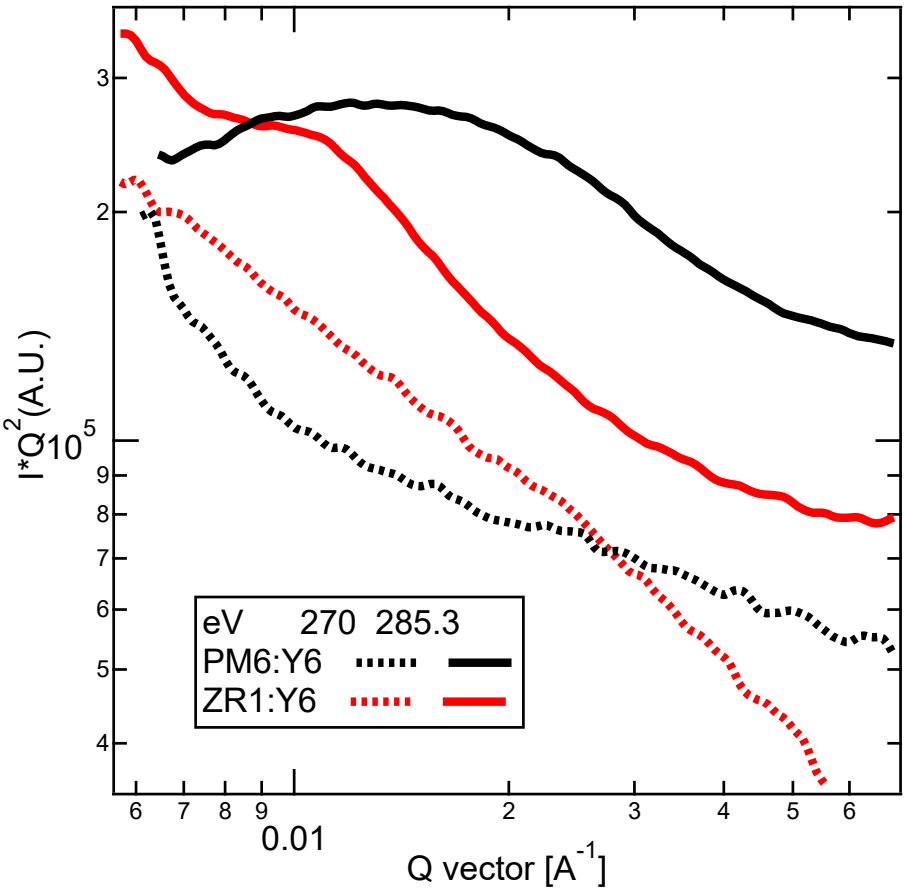

Figure S11. *1D RSoXS profiles of PM6:Y6 blend (black curves) and ZR1:Y6 blend (red curves). Dotted curves are acquired at X-ray energy of 270 eV (non-resonant, multiplied by 2.5x) and solid are acquired near resonant energy (at 285.3 eV). The characteristic length (Lc) which is an indicator of domain size and can be estimated as 2*pi over q* (where q* is the feature position of an RSoXS profile). The domain purity is proportional to the total scattering intensity, which is the area under an RSoXS curve.*

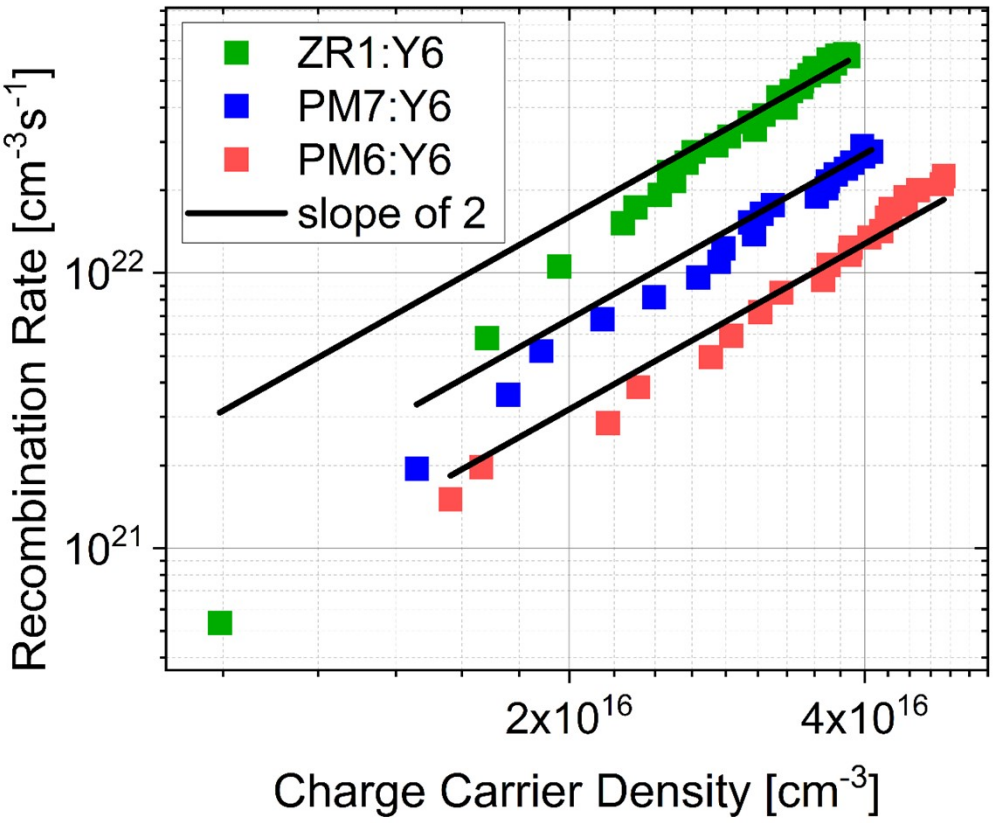

Figure S12. *Recombination rates for the PM6:Y6, PM7:Y6, and ZR1:Y6 devices under V_{OC} conditions are plotted against the collected charge carrier density in response to 2.07 eV light excitation. The data are shown in a double-log scale (scatter plots) with reference lines indicating a slope of 2, representing the ideal recombination rate coefficient.*